EVALUATION OF WATER SATURATION FROM RESISTIVITY IN A CARBONATE FIELD. FROM LABORATORY TO LOGS.

M. Fleury [1] , M. Efnik[2] , M.Z. Kalam[2]

(1) Institut Français du Pétrole, Rueil-Malmaison, France
(2) ADCO, Abu Dhabi, UAE

This paper was prepared for presentation at the International Symposium of the Society of Core Analysts held in Abu Dhabi, UAE, 5-9 October 2004

ABSTRACT

We present an extensive laboratory study to determine initial water saturation as well as remaining oil in water flooded regions in a carbonate field. The impact of the laboratory results for the well and for the reservoir is also considered.
The entire sequence necessary for the log calibration has been studied in the laboratory: brine resistivity, formation factor at overburden stress and reservoir temperature, resistivity index (RI) curves in drainage and imbibition at reservoir conditions. The formation factor can be described using a unique Archie law for all rock types. The RI curves are much more complex and variable and can often not be described by a simple Archie law.
The initial water saturation was estimated using the RI curves in drainage. Very low saturation was reached covering the range of saturation of interest in the field; n values around 1.7 are typical. In imbibition, a strong hysteresis was generally observed and RI curves are strongly non-linear in log-log scale with typical n values of 2.5 at high saturation. Therefore, the log calibration in water flooded regions must be performed using different curves. A calibration methodology for non-Archie RI curves is presented.
Despite mixed- wet conditions, n values are lower than the default value of 2 and much lower than expected in strong oil wet conditions. When considering the saturation range [0.05 – 0.2], the choice of an appropriate n value is critical. For the water-flooded regions, the existence of a drainage-imbibition hysteresis has severe consequences on the evaluation of water saturation. In general, the laboratory measurements reduced the uncertainties in the oil in place estimations and allowed a realistic evaluation of the water flooding performance.

INTRODUCTION

A key information in formation evaluation is the oil in place. It depends on the volume of the reservoir, the porosity and the saturation. For reservoirs produced for many years using a large number of wells, the uncertainties linked to the volume of the reservoir is very small. The porosity may also be known quite precisely using logs and inexpensive core data without much difficulty. Finally, the saturation estimated from resistivity logs

can be a significant source of uncertainties due to the complexity of the electrical response in carbonates. For water flooded reservoir, the second key information is the estimation of the water saturation after flooding.
To tackle the above issues, an extensive experimental program was conducted using a dedicated well. The more advanced techniques for core preservation were used under appropriate drilling conditions. Beside the acquisition of data for log calibration, specific tests were planned to compare ambient and reservoir condition measurements, and evaluate the effect of live oil compared to dead oil. Finally, a complete set of data was obtained covering the entire reservoir.

GENERAL APPROACH

All the steps necessary to calibrate the resistivity logs were performed: formation water resistivity (Rw), formation factor (FF) and resistivity index (RI) measurements. The effect of the main parameters influencing the resistivity were studied independently: the effect of stress was studied on the formation factor, and the effect of wettability on the resistivity index. For the latter, a pre-study was first performed to estimate the effect of measurement conditions and decide which of them are more appropriate: ambient conditions with refined oil, reservoir temperature with dead oil, reservoir temperature with live oil.
Since the reservoir has been water flooded for nearly 30 years, a key data is the determination of the imbibition RI curves to estimate the water saturation in flooded zones. Classically, the main uncertainty when calibrating water flooded zones comes from the water salinity. However, in the present situation, the injected water originates from a nearby aquifer of similar salinity. The imbibition RI curves were systematically measured because of the possible existence of hysteresis between drainage and imbibition. The underlying physics of this hysteresis is not well understood and is presumably associated with the wettability (mixed-wet or moderately oil wet) of the pore medium.
We used the existing reservoir rock type (RRT) classification as a base for selecting the sample for formation factor and resistivity index measurements. For each RRT, a minimum of two samples was chosen. The 7 RRT classes are essentially based on permeability (RRT7<0.1 mD, RRT6<1 mD, RRT5< 5mD, RRT4<25 mD, RRT3<100 mD, RRT2<500 mD, RRT1>500 mD). There is no systematic variation of porosity among the different RRTs and permeability is not correlated with porosity as often observed in carbonates. The high permeability RRTs are the most heterogeneous ones and are characterized by a bimodal or wide pore body/throat size distribution as indicated by NMR and mercury injection. However, in terms of accumulation, they only represent about 10 %. The medium permeability RRTs (3,4 and 5) contain most of the oil in place.

SAMPLE PREPARATION AND EXPERIMENTAL METHODOLOGY

Sample preparation

All plug samples were extracted from one well for which a special attention was given in terms of coring and preservation (water based mud). After reception of the full size cores, the plugs were drilled and cleaned using an optimized procedure in order to render the samples as water wet as possible. USBM tests indicate that the wettability after cleaning is between +0.1 and +0.5.

The samples were systematically characterized using NMR low field techniques. Therefore, the drying step necessary to determine pore volumes can be omitted. This has the advantage of not destabilizing the pore surface. Instead, the pore volumes (Vp) were determined directly by NMR using a specific procedure to avoid hydrogen index corrections as well as others errors induced by the imperfection of the instrument. Note that the NMR Vp will catch all components of the porosity, including microporosity that can be difficult to dry. For vuggy samples, a sleeve was kept around the sample in order to keep the vugs filled with water. When too large, they were filled with cement.

Fluids

The reservoir brine was reconstituted following a water analysis performed earlier (a total of 150 gr/l of various salts). The resistivity ρ_w of the brine at reservoir temperature is calculated from the measured resistivity at laboratory temperature using the following relation (Arps relation) :

$$\rho_w(T_2) = \rho_w(T_1)\ \frac{T_1 + 21.7}{T_2 + 21.7} \tag{5}$$

where T_1 and T_2 are expressed in °C. The reference temperature of the reservoir is 121°C, at which all reservoir condition experiments were performed. At reservoir temperature, Rw=0.0183 Ω.m.

The oil of this field is light (API>35). For dead oil experiments, the stock tank oil was filtered at 10 μm before use. The dead oil/brine interfacial tension at 20°C is 21 mN/m.

Resistivity measurements

For the formation factor and resistivity index experiments, the electrical resistance of the sample is measured using an HP4263 RLC meter combined with an (in-house) isolator to avoid ground problems. The impedance meter measures the voltage drop occurring when a current is circulating through the sample (frequency=1 kHz, peak to peak voltage=500 mV). The resistance of the sample is deduced from the real part of the signal. In all cases, the acquisition line is checked before starting an experiment by replacing the sample by a set of calibrated resistors that includes if necessary contact resistances.

Formation factor measurements

For these experiments, the resistance and pore volume variations are recorded as a function of time and confining pressure (triaxial stress). The pore pressure is kept constant (10 bar). In addition, the permeability is measured at the minimum and

maximum confining pressure as a quality check. The resistance of the sample (L=6 cm, D=4 cm) was measured using a two-electrode principle in which the face end-pieces are used as current and voltage electrodes. The variation of pore volume was measured using a thin tube that allows a very accurate determination of volume variations (sensitivity=0.002 cm3, accuracy=0.01 cm3). The porosity at different net overburden pressures P is obtained by taking into account the initial NMR pore volume and the measured volume of fluid ΔV expelled from the sample at each confining pressure step:

$$\Phi(P) = \frac{Vp - \Delta V(P)}{Vt} \quad (1)$$

For a given confining pressure, the formation factor FF is plotted as a function of porosity assuming Archie's law:

$$FF = a\phi^{-m} \quad \text{where} \quad FF = \frac{\rho_S}{\rho_w} \quad \text{and} \quad \rho_S = R_S \frac{S}{L} \quad (2)$$

where ρ_S and ρ_w are respectively the resistivity of the sample and of the brine at reservoir temperature (121°C), S is the surface area and L the length of the sample and R_s the measured resistance of the core sample.

For each confining pressure step, we used the measured resistance to control the stability of the system (Figure 1). The stability is obtained faster at low confining pressure (after 5 hours) than at high confining pressure (after 20 hours). For all the samples, the confining pressure was changed after examination of the resistance curve.

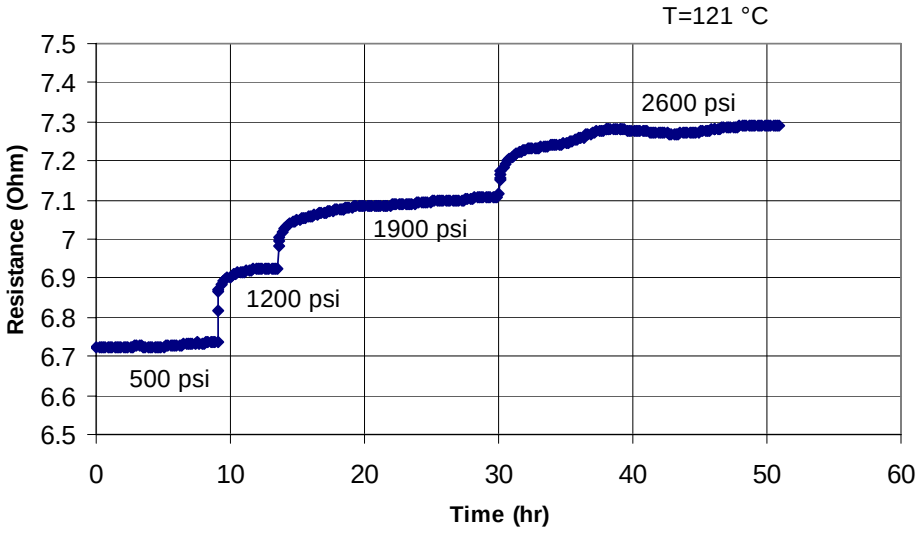

Figure 1: example of measurement of the resistance of a sample for different confining pressures. The oscillations at 2600 psi are due to temperature fluctuations of the oven.

Resistivity index measurements

The experiments were performed using a four-electrode principle to avoid contact resistance, and a semi-permeable ceramic filter (« porous plate ») at one face of the sample in order to impose a given oil-water differential pressure (capillary pressure). Resistivity, water production, various pressures and various temperatures are monitored

continuously. For each oil-water pressure difference, a point on the resistivity index curve (RI=Rs(Sw)/Rs(Sw=1)) and drainage capillary pressure curves is obtained when the saturation is stabilized (Figure 2). The duration of such an experiment is typically 1000 hours. For all experiments, at least one pressure step is kept longer than necessary in order to verify the stability of the volume measurements (Figure 2, t=800 hr, even a very small leak during a long period can generate large errors). The largest capillary pressure applied is 4 bar at reservoir conditions. This was enough to reach very small saturation, even for low permeability samples.

In order to study the influence of live oil, a special end-piece was designed in order to be able to remove the ceramic filter while keeping the confining pressure and perform a flooding with live crude oil. This operation was performed on a few samples at irreducible saturation at the end of the drainage with dead oil. The live oil flooding was then performed during one week at low flow rate and the resistance monitored in order to observe indirectly the possible change of fluid distribution and wettability associated with live oil vs. dead oil. No water production was observed during the live oil flooding.

The imbibition saturation exponent measurements have been performed by injecting reservoir brine at constant flow rate through the sample (and through the ceramic). The resistance of the sample was monitored continuously and the saturation measured at regular intervals at the oil-water separator. The procedure used minimizes the impact of dead volumes. The laboratory flow rates are between 0.1 and 10 cc/h to cover the largest possible saturation range. The corresponding field rates are between 0.2 and 3 ft/day.

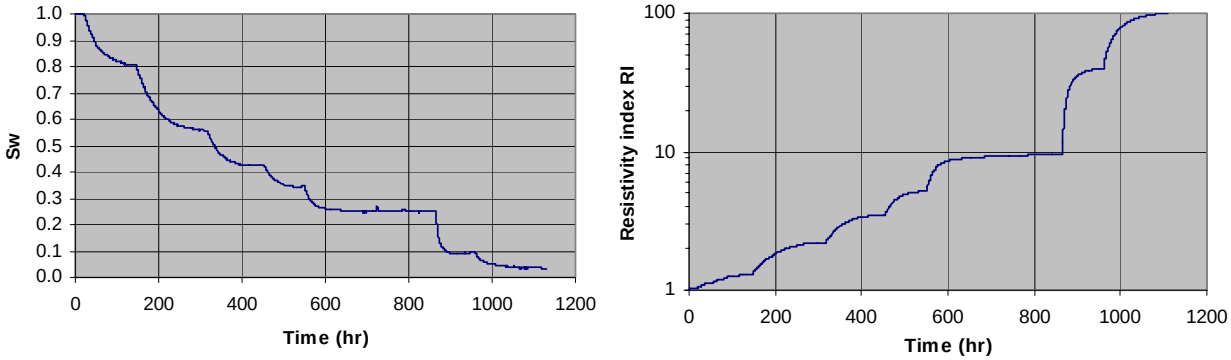

Figure 2: example of measurements of saturation and resistivity index. The equilibrium data points are used to build the RI and Pc curves. The pressure steps are successively: 0.058, 0.164, 0.266, 0.383, 0.495, 0.680, 1.455 and 2.465 bar. Measurement condition: T=121°C, dead oil, overburden pressure 30 bar. Sample: Kw=21.9 mD, Φ=0.289.

RESULTS

Cementation exponent

The formation factor has been measured at reservoir temperature (121°C) on 14 samples from rock types RRT1 to RRT7, covering the depth interval of the reservoir, as a function of net overburden pressure in the range [25 – 170 bar, 360 – 2460 psi]. The highest value

(170 Bar) corresponds to the estimated in-situ effective stress The data points from all RRTs follow an Archie law with a good correlation (Figure 3):

$$FF = 0.721\Phi^{-2.242} \quad \text{T=121°C}, \quad 0.05<\Phi<0.34 \qquad (3)$$

In addition, it was found that the formation factor does not depend significantly on the net overburden pressure (a=0.95, m=2.04 at P=25 bar) even for vuggy samples and that m values measured at ambient conditions can be used for log calibration with a reasonable accuracy. In fact, the variation of porosity and resistivity are compensating each other, yielding a quasi-constant formation factor.

To correct routine porosity and water permeability measurements, we also established during the formation factor measurements the useful following relationships:

$$\Phi(P=170Bar) = 0.954\Phi(P=25Bar) + 0.484 \quad \text{at T=121°C} \qquad (4)$$

$$kw(P=170Bar) = 0.948kw(P=25Bar)^{0.958} \quad \text{at T=121°C} \qquad (5)$$

Note that brine permeability is reduced by about 35% for RRT1 when the confining stress is increased. This effect tends to be gradually smaller when deeper or less vugular RRTs are considered.

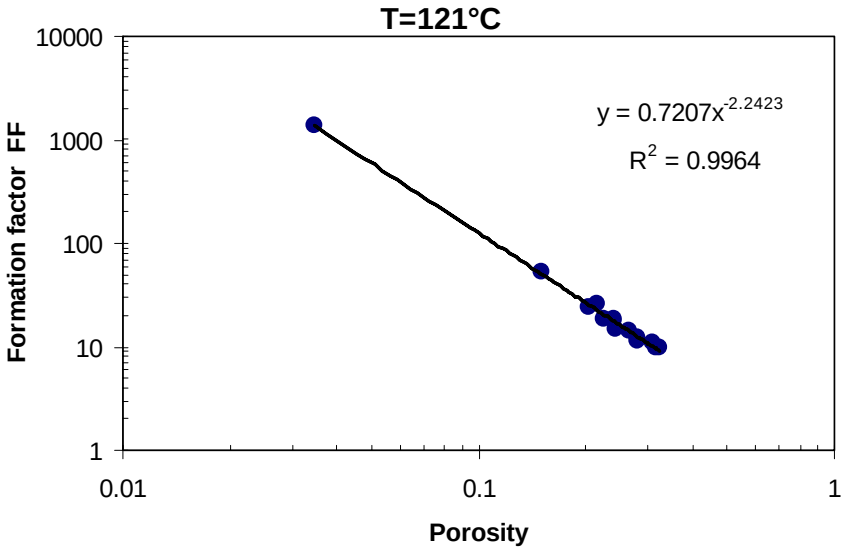

Figure 3: Formation factor FF at reservoir temperature and maximum net overburden pressure (170 Bar, 2460 psi). The correlation law is valid at the highest confining pressure representative of in-situ stress.

It is surprising to observe that the formation factor results are close to those obtained in sandstones. From long established literature, (Winsauer et al. 1952 and others), a typical relationship in sands is $FF = 0.62\Phi^{-2.15}$. This relation is also often cited in textbooks for consolidated sandstones. The weak sensitivity to stress is also a behavior characterizing more sandstones than carbonates. In contrast, Focke et al. (1987) observed variations between rock types and recommended to measure m for each of them, as performed in this study. Recent measurements performed by the first author as well as recent litterature review (Ragland, 2002) confirmed that the formation factor can deviate largely from an Archie law. In the present case, a unique relationship is found for all rock types

in a wide range of porosity, greatly simplifying the interpretation of resistivity logs, as well as increasing the accuracy of water saturation calculation. It is also in agreement with previous studies performed on the same field (Longeron and Yahya, 1991). But this result should not be considered as general.

Drainage RI curves

Drainage-imbibition RI curves were measured on 14 samples from all rock types. In general, Sw smaller than 10% were reached and sometimes as low as 3%. For these unusual low values, we double-checked all volume measurement (NMR pore volume, production, dead volumes, etc). Such low value can also be reached by centrifuging similar samples at the same capillary pressure. For some samples, the measurements have been performed on the cleaned sample first at ambient conditions using refined oil and then at reservoir conditions (not shown here). We concluded that reservoir conditions were necessary to reduce the uncertainties.

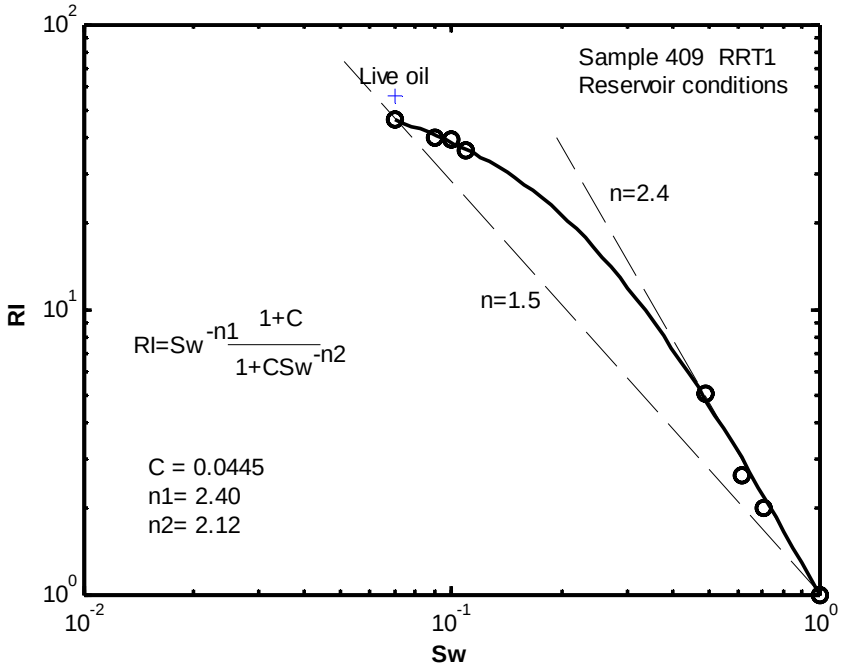

Figure 4: Typical result for vugular samples from RRT1. The curve is bending down at low saturation. The use of n values deduced from the high saturation range lead to severe errors. The cross indicates the resistivity index measured after flooding with live oil.

Two examples of measurements are given in Figure 4 and Figure 5. For the most heterogeneous rock type (RRT1), non-standard behaviors were found. The measured RI curve is not a simple Archie law but can be described by the following semi-empirical law (Fleury, 2003):

$$RI = Sw^{-n1}\frac{1+C}{1+CSw^{-n2}} \qquad (6)$$

The origin of this behavior is thought to be due to a short-cut effect associated with the smallest pore population, as described in Fleury (2002). A curvature was also observed in

some of the tight samples from RRT 6 and 7, for which the microporosity (NMR T_2<10 ms) can represent more than 10% of the total porosity. Whatever the physical explanation, the impact on log calibration is huge. Taking the saturation exponent measured at high saturation (n_1=2.4, Figure 4), a water saturation of 0.2 is deduced at RI=50 instead of a saturation of 0.05.

An example of the effect of live oil at the end of drainage is shown in Figure 4. The variation of resistance while injecting live oil was observed during one week and resulted in a small increase of RI. In three other cases, a similar or negligible increase was observed. The use of live oil has a small effect in the present system and can be considered as a second order effect compared to the variability generated by the samples or rock types themselves, as will be seen later.

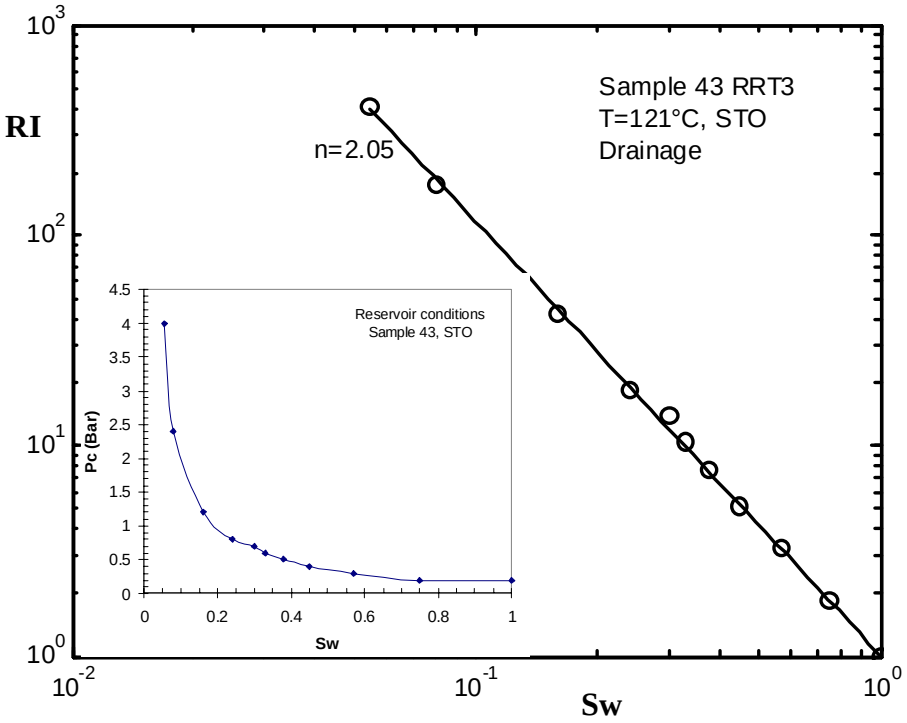

Figure 5: An example of measurement for the RTT3. An Archie law is found down to Sw=0.05.

However, standard Archie laws were found in most cases (10/14 e.g. Figure 5) down to very low saturation. Note that RI curves at low saturation (<0.1) are very sensitive to small errors in the pore volumes. The example shown concerns one of the dominant RRT. We summarize the results in Figure 6. The 14 measured RI curves can be reduced to a set of 8 curves representing all rock types, except for RRT5 for which the two available measurements gave very different results (n=1.4 and 2.05) for non-obvious reasons. For all other RRTs, the RI curves were similar and within the experimental uncertainties. When considering this reduced set of curves, we observe a large variability of the saturation exponent n. At a saturation of 0.05, the resistivity index can vary by one order of magnitude. In other terms, the saturation exponent varies from around 2 down to 1.5.

A dependence with the rock type was not found. Instead, a dependence with the amount of microporosity as detected by NMR was searched but this did not lead to satisfying predictions. For the RRT 5, two very different curves were found (5a and 5b, Figure 6). Note that the variability on n is in contrast with the uniform results obtained on the formation factor.

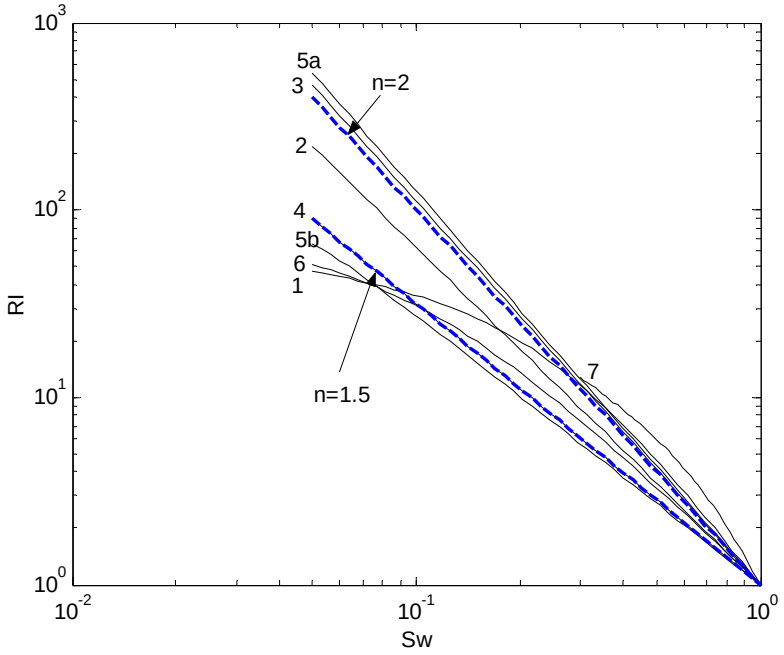

Figure 6: Summary of all drainage RI curves. For clarity, the fitted curves according to equation 6 are plotted excluding the data points down a single final saturation of 0.05, except for RRT7 for which the final saturation was very different (Sw=0.3).

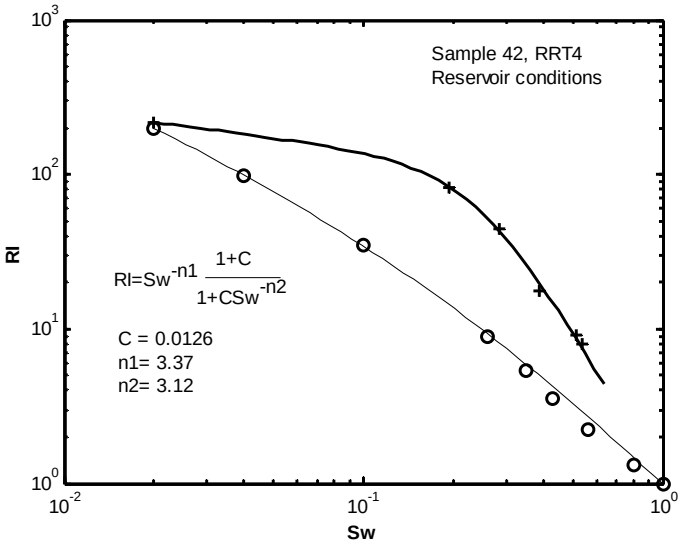

Figure 7: Typical example of imbibition RI curve.

Imbibition RI curves

In imbibition, a strong hysteresis was found in most cases (11/14). We used the equation 6 to model the data points (Figure 7), allowing a easy interpolation between data points and an extrapolation up to Sw=1. Essentially, RI is weakly sensitive to saturation below 0.2 and very sensitive to saturation in the range of interest in the field (around Sw=0.5, 2<n<3.5, Figure 8). This hysteresis has a large impact on log data calibration. It has not been evidenced in the past systematically. The general belief among researchers is that an hysteresis between drainage and imbibition may occur when the rock is not water-wet. Intuitively, the absence of resistivity hysteresis would be surprising in the presence of the strong hysteresis in the capillary pressure curves but a detailed understanding or description of the mechanism involved is still lacking.

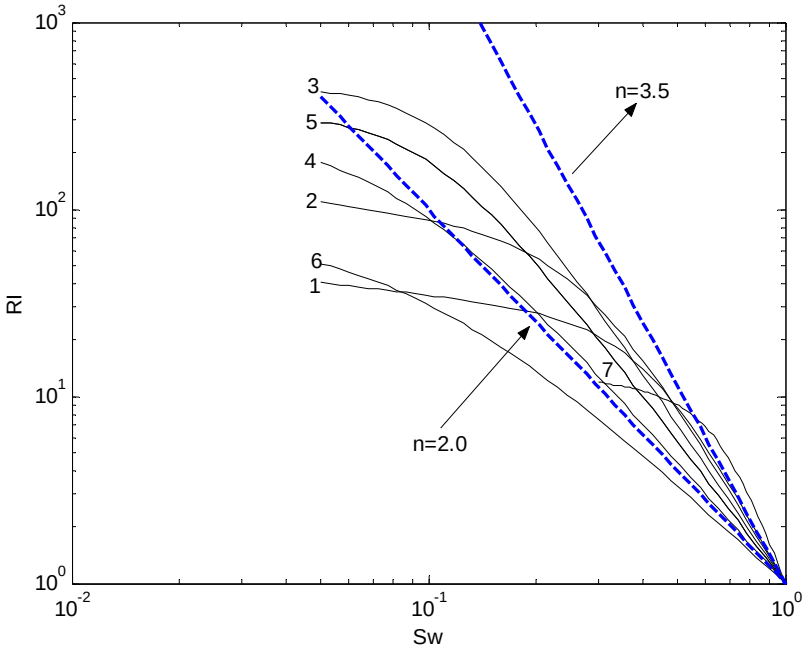

Figure 8: Summary of all imbibition RI curves. For clarity, the fitted curves are plotted excluding the data points up to Sw=1. The saturation reached during the experiments was around Sw=0.5.

IMPACT ON LOG CALIBRATION

We calibrated the resistivity log of the well from which the samples are coming using the laboratory measurements. The following steps were applied:

1) Calculate Ro as a function of depth using:

$$Ro = FF\ \rho w = a\Phi^{-m}\rho w$$

where ρw=0.0183 Ω.m , a=0.721, m=2.24, Φ is the log density neutron porosity slightly corrected to match core measurements,

2) Calculate the resistivity index as a function of depth using:

$$RI = \frac{Rt}{Ro}$$

where Rt the AIT90 corrected log resistivity,

3) Calculate saturation as a function of depth using:

$$Sw = RI^{1/n} \text{ for Archie RI curves }, \; Sw = \exp\left[\sum_{i=1}^{4} A_i \log(RI)^i\right] \text{ otherwise}$$

where the coefficient Ai are fitted on a given RI(Sw) curve (the above summation is a convenient way to invert the RI(Sw) relationship).

The result after step 2 is shown on Figure 9. The plot of the log resistivity index vs. depth gives a useful overview of the saturation independently of porosity and allows an estimation of water saturation if one uses the laboratory results plotted in Figure 6 and Figure 8. In non water flooded zones (170 – 300 ft), RI is of the order of 100 in agreement with the laboratory measurement at a saturation of about 10 %. Note also that RI can fluctuate by a factor of 10 even at the resolution of the logging tools. They are due either to saturation fluctuations or to fluctuations of electrical properties of the porous medium (such as n=1.5 or n=2.0).

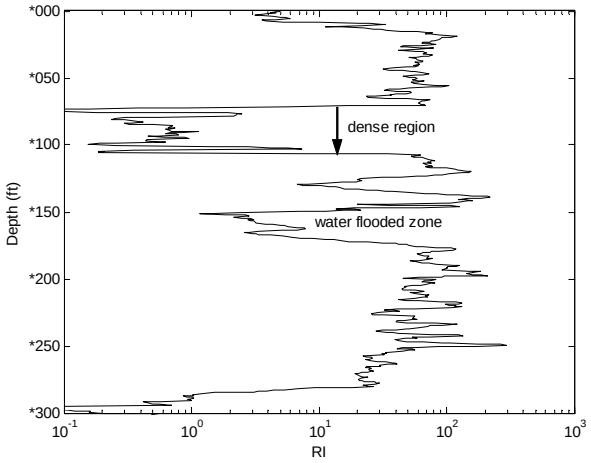

Figure 9: Log resistivity index calculated using the measured Rw and formation factor. The water flooded zone appears clearly as low RI value at depth 150. Outside this zone, the RI values are of the order of 100, in agreement with laboratory measurements.

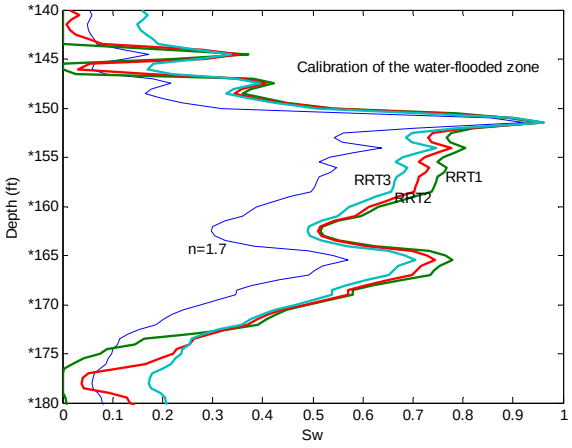

Figure 10: Calculation of water saturation in the water flooded zone. We used the neutron-density porosity and the inverse RI(Sw) relationships established in the laboratory.

The results after step 3 are shown in Figure 10 for the water-flooded zone. In this case, it is essential to take into account the non-Archie behavior of the RI curves. We assume here that the resistivity Rw of the injected water is not different from the initial water. This assumption is reasonable because the injected water originates from a nearby

aquifer. As an example, we show the calculated saturation using a drainage type Archie law with n=1.7 (a medium slope characterizing drainage curves), and using the RI curves obtained on RRT1, RRT2 and RRT3. A wrong RI calibration would lead to the conclusion of a very poor water flooding efficiency, while the use of the proposed hysteresis model lead to the opposite conclusion, a reasonably efficient flooding.

CONCLUSIONS

Formation factor and resistivity index were measured on seven rock types (RRT) representing the entire reservoir. The formation factor measurements determined at reservoir stress could be described using a unique Archie law including all RRTs. The resistivity index curves measured in drainage at reservoir temperature with dead oil were much more variable and the saturation exponent n varied from 1.4 to 2.1. For heterogeneous rock types or samples having a large amount of microporosity, the RI-Sw relationship is not a power law and a new model was used to describe the data. For all rock types except the tighter one, low saturation (<10%) representative of field values were reached. The main remaining difficulty is to link the electrical response to the appropriate structural parameters of the rock.

The most important effect lies in the strong difference between drainage and imbibition resistivity index curves, also modelled by a novel resistivity equation. The resistivity index has been found to be much larger in imbibition than in drainage, implying a severe underestimation of the water saturation if the drainage curve is taken instead, as usual. For non-Archie curves, the inverse relationship Sw=fct(RI) should be fitted to laboratory data in order to facilitate the log processing.

ACKNOWLEDGMENTS

The authors wish to acknowledge ADCO for permission to publish this work.

REFERENCES

1. Fleury M., 2002, "Resistivity in carbonates: new insights", Proceeding of the International Symposium of the Society of Core Analysts, Monterey, 22-25 September.
2. Fleury M., 'Advances in Resistivity Measurements using the FRIM Method at Reservoir Conditions. Applications to Carbonates.' Proceedings of the International Symposium of the Society of Core Analysts, September 2003, Pau, FRANCE.
3. Focke J.W. and D. Munn, ‘Cementation Exponents in middle Eastern Carbonate Reservoirs’, SPE Formation Evaluation, SPE 13735, June 1987.
4. Longeron D. and F. Yahya, Proceeding of the International Symposium of the Society of Core Analysts, paper 9117, 1991.
5. Ragland D., 'Trend in cementation exponents (m) for carbonate pore systems', Petrophysics, Vol. 43, N°5, Sept. 2002.
6. Winsauer, W.O. et al . : ‘Resistivity of brine saturated sands in relation to pore geometry’ Bull. AAPG (1952), 36, 253-77.